Biomaterials Science

Bisphosphonate-Functionalized Hyaluronic Acid Show Selective Affinity For Osteoclasts As A Potential Treatment For Osteoporosis

Journal:	*Biomaterials Science*
Manuscript ID:	BM-ART-03-2015-000096.R1
Article Type:	Paper
Date Submitted by the Author:	27-May-2015
Complete List of Authors:	Kootala, Sujit; Uppsala University, Polymer Chemistry Ossipov, Dmitri; Uppsala University, van den beucken, jeroen jjp; Radboudumc, Biomaterials (309) leeuwenburgh, sander; Radboudumc, Biomaterials Hilborn, Jöns; Uppsala University, Material Chemistry

Biomaterials Science

ARTICLE

Bisphosphonate-Functionalized Hyaluronic Acid Show Selective Affinity For Osteoclasts As A Potential Treatment For Osteoporosis

Received 00th January 20xx,
Accepted 00th January 20xx

DOI: 10.1039/x0xx00000x

www.rsc.org/

Sujit Kootala, MS[1] Dmitri Ossipov, Phd[1], Jeroen JJP van den Beucken, Phd[2], Sander Leeuwenburgh, Phd[2], Jöns Hilborn, Phd[1]

Current treatments for osteoporosis involve administration of high doses of bisphosphonates (BPs) over a number of years. However, the efficiency of absorption of these drugs and specificity towards target osteoclastic cells is still suboptimal. In this study, we have exploited the natural affinity of high- (H) and low- (L) molecular-weight hyaluronic acid (HA) towards cluster of differentiation 44 (CD44) receptors on osteoclasts to use it as a biodegradable targeting vehicle. We covalently bound BP to functionalised HA (HA-BP) and found that HA-BP conjugates were highly specific to osteoclastic cells and reduced mature osteoclast numbers significantly more than free BP. To study the uptake of HA-BP, we fluorescently derivatised the polymer-drug with fluorescein B isothiocyanate (FITC) and found that L-HA-BP could seamlessly enter osteoclastic cells. Alternatively, we tested polyvinyl alcohol (PVA) as a synthetic polymer delivery vehicle using similar chemistry to link BP and found that osteoclast numbers did not reduce in the same way. These findings could pave the way for biodegradable polymers to be used as vehicles for targeted delivery of anti-osteoporotic drugs

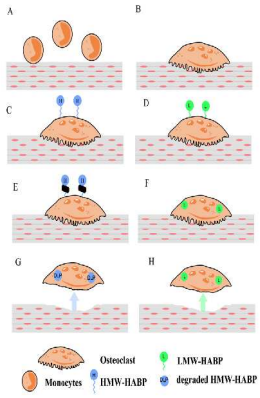

[1]Department of Chemistry, A Science for Life Laboratory, Polymer Chemistry Division, Uppsala University, Po Box 538, Lägerhyddsvägen 1, Uppsala SE 75121, Sweden.
[2]Department of Biomaterials, Radboud umc (309), PO Box 9101, 6500 HB Nijmegen, The Netherlands.
Corresponding Author: Prof. Jöns Hilborn, [1]Department of Chemistry, Polymer Chemistry Division, Uppsala University, Po Box 538, Lägerhyddsvägen 1, Uppsala SE 75121, Sweden. Tel: 018-471 3839 Fax: 018-471 3477 Email: Jons.Hilborn@kemi.uu.se
Electronic Supplementary Information (ESI) available: [details of any supplementary information available should be included here]. See DOI: 10.1039/x0xx00000x

A. Introduction

Osteoporosis involves major physiological changes in bone, rendering it porous and brittle. As such, osteoporosis is a major health concern in developed countries and affects 20% of males and 30% of females worldwide, particularly at the postmenopausal age.(*1, 2*) Approximately 9 million fractures occur each year worldwide on account of osteoporosis and 30% of these occur in the EU.(*3*) It is projected that by 2025, in the US alone, the economic burden of treating osteoporosis-related fractures will exceed $25 billion.(*4*) Hence, improved treatments would be of considerable societal and economical value.

Bone can be referred to as either a tissue or an organ; it is composed of a complex three-dimensional multicellular structure. Healthy bone entails a fine balance between osteoblasts, osteocytes and osteoclasts, which are the three major cell types required for the continuous turnover of bone.(*5-7*) Osteoblasts are responsible for the deposition of new hydroxyapatite bone mineral and form osteocytes after becoming embedded in the deposited extracellular matrix.(*8*) These osteoblasts express alkaline phosphatase (ALP), type 1 collagen, RUNX2 and osteocalcin that are used as major indicators of mature functioning osteoblasts.(*9*) Osteoclasts are responsible for bone resorption and appear as large multinucleated cells with ruffled borders that attach to the mineralised extracellular matrix, degrade it and release free calcium into the blood in a process that allows continuous remodelling of bone.(*10*) These osteoclasts arise from the hematopoietic lineage (i.e. monocytes/macrophages) and express tartrate-resistant acid phosphatase (TRAP), cathepsin K and vitronectin receptor as markers indicating maturity.(*11-13*)

Osteoporosis is associated with insufficient bone formation and a highly active population of osteoclasts, thereby causing excessive calcium resorption that cannot be naturally compensated by mineralising osteoblasts. Osteoblasts exert control over osteoclasts through the secretion of receptor activator of nuclear factor kappa B ligand (RANKL),(*14, 15*) which along with macrophage colony stimulating factor (M-CSF) as key factors responsible for the differentiation of monocytes into osteoclasts.(*16*) Osteoblasts also control the number of osteoclasts through secretion of osteoprotegerin (OPG), a member of the tumour necrosis factor (TNF) receptor superfamily.(*17*) Together, these signalling molecules maintain a healthy balance of the overall number of osteoclasts and osteoblasts. Current clinical strategies for the treatment of osteoporosis focus on restoring the balance between mineralisation and resorption by administering drugs to reduce osteoclast numbers, thereby reducing the overall rate of resorption.(*18, 19*) The most common family of anti-osteoporotic drugs are bisphosphonates (BP's) that primarily act to reduce osteoclast numbers. Alternatively, glucocorticoid-based therapies such as parathyroid hormone or oestrogen (with or without progesterone) that stimulate osteoblast activity are used to counterbalance increased bone resorption.(*3, 20, 21*) BP's are analogues of inorganic pyrophosphates and comprise two phosphonate groups bridged through a common carbon atom. Similar to inorganic phosphates, phosphonate groups account for the chelation of calcium ions.(*22*) This effect renders bone the most abundant target for BP's, specifically under the conditions of bone resorption when large amounts of calcium are released from bone tissue. Four generations of BP's have been developed since the introduction of the first BP's, presenting increased efficacy profiles and mode of delivery. They are broadly classified as amino and non-amino BP's. Zoledronate and risedronate have proven to be the most potent BP's.(*23*) Zoledronate has shown superior potency in terms of anti-osteoclastic behaviour, mainly due to the involvement of the amino group located on one of its two side groups.(*22*) Another parallel strategy advocates that modifying the second side group of BP's with an amine likewise results in enhanced action against osteoclasts. The essential condition for the pharmacological activity of BP's is the acidic microenvironment in the resorption lacunae that is created by mature functioning osteoclasts.(*24*) Since BP's bind to the mineral in bone, acidic conditions result in the protonation of the phosphonate groups to trigger release of the BP moiety from the matrix. The osteoclasts absorb the released BP through the endocytic pathway and release it into the cellular compartment as they encounter the acidic environment of the vesicles. Once released intracellularly, amino BP's inhibit farnesyl diphosphate synthase, a key enzyme involved in the synthesis of cholesterol.(*25*) This inhibition is known to affect the prenylation of GTPase signalling proteins, which affects the ability of the osteoclasts to anchor themselves to the surrounding matrix. The entire process results in major disruptions in the functioning of mature osteoclasts involving attachment and presentation of the ruffled membrane borders necessary for resorption.(*26*) Eventually, because of the inability of osteoclasts to anchor and resorb, they undergo apoptosis, leading to a reduction in their overall numbers.

BPs may be administered either orally or intravenously. Oral administration has the disadvantage of diminished bioavailability over time, necessitating multiple sessions of administration.(*27*) Comparatively, intravenous administration of BP's has resulted in stronger and longer lasting anti-resorptive effects. However, because of issues such as poor compliance, persistence of continued therapy, dosage issues and continued use of BP's, the dropout ratio of patients is as high as 50%, resulting in poor patient recovery outcomes.(*28*) The main reason for discontinuing oral administration is gastrointestinal complications driving patients to discontinue their treatment midway.(*29*) Another issue with BP's relates to osteonecrosis of the jawbone, which has been shown to become apparent upon cancer treatment with (high doses of) BP's.(*30, 31*) Therefore, strategies to increase the therapeutic and targeting efficiency of BP's towards osteoclasts to reduce the dosage of BP's would be highly beneficial for the treatment of osteoporosis.

Particularly, BP's adsorb onto the surface of bone to provide release of BP's as the HAP is resorbed along with the adsorbed BP's, allowing osteoclast inhibition over an extended period.(35) To change the pharmacokinetic properties of BP's, they have also been linked to polyethylene glycol (PEG) that is known to escape protein interactions. PEG-alendronate conjugates in osteoporotic rats have been shown to effectively inhibit the decrease in the width of the growth plate in bone to a level achieved with intrapulmonary administration of alendronate alone in an effort to reduce the side effects of alendronate on the mucosal and gastric lining, however not necessarily increasing the efficiency of the drug.(36) In another study, alendronate was linked to poly(D,L-lactide-co-glycolide) (PLGA) to determine if the drug retained its anti-osteoclastic properties after the conjugation [ref]. However, the experiments showed that the PLGA-alendronate conjugate had no better anti-osteoclastic properties than PLGA alone.(*32*) Hence, methods to enhance the targeting of BPs to osteoclastic cells to improve BP efficacy and reduce BP side effects are currently not available.

Hyaluronic acid (HA) is a non-sulphated glycosaminoglycan that comprises repetitive disaccharide units consisting of monomers of *N*-acetyl-D-glucosamine and D-glucuronic acid and forms a linear polysaccharide chain.(*33*) It is an essential developmental molecule

found in many parts of the human body, such as the synovial cavities, eyes, umbilical cord and connective tissues. HA is synthesised and degraded in vivo, assisted by hyaluronan synthases and hyaluronidases, respectively.(*34*) Amongst others, the cluster of differentiation 44 (CD44) receptor-mediated pathway is the major route for entry of HA into the cells and is recognised by specific enzymes, hyaluronidases, for extracellular and intracellular degradation.(*35*) HA shows high affinity to CD44 receptors on the cell surface and undergoes CD44-mediated endocytosis in osteoclasts but not in osteoblasts.(*36*)

The purpose of this study was to test the hypothesis that covalent coupling of HA to BP increases its affinity towards osteoclasts in comparison to osteoblasts in vitro, thereby enhancing the targeting ability of the drug. We derivatised HA with BP (pamidronate) and in order to follow the cellular delivery, labelled the polymer with a fluorescent tag. We found that HA by itself could assist the preferential uptake into osteoclasts, in contrast to osteoblasts, to provide higher potency of the BP-linked adduct than the free drug. We believe that this is the first step towards developing an effective targeting strategy for BP's to enhance its specificity and lower the required doses.

B. Materials and Methods

Synthesis of HA-thiol (HA-SH) derivatives. HA (400 mg, average MW 8000 Da, 1 mmol of disaccharide units) was dissolved in 40 mL of deionised water. Dihydrazide linker **1** (35.7 mg, 0.15 mmol) was added to the HA solution. *N*-hydroxybenzotriazole (HOBt, 153 mg, 1 mmol) was separately dissolved in 6 mL of acetonitrile:water mixture (v/v = 1:1) and added to the HA solution. The pH of the resultant solution was adjusted to 4.7, after which the coupling reaction was initiated by addition of solid 1-ethyl-3-(3-dimethylaminopropyl)-carbodiimide (EDC, 96 mg, 0.5 mmol) to the reaction mixture. The mixture was stirred overnight and then basified to 8.5 with 1 M NaOH. DL-dithiothreitol (DTT, 116 mg, 0.75 mmol) was added to the solution. The mixture was stirred overnight, after which the solution was transferred to a dialysis tube (MW cutoff = 3500). After exhaustive dialysis against dilute HCl (pH 3.5) containing 0.1 M NaCl, followed by dialysis against dilute HCl (pH 3.5) two times, the dialysed solution was lyophilised to give 214 mg of low-molecular-weight (L-HA) thiol-modified HA (54% yield). The degree of incorporation of thiol (10%, of the disaccharide repeat units) groups in L-HA HA-SH was verified by comparison of integration of the $-CH_2CH_2SH$ side chain peaks at 2.58 and 2.73 ppm with the acetamido moiety of the *N*-acetyl-D-glucosamine residue of HA. High-molecular weight (H-HA) thiol-modified HA was synthesised analogously from 400 mg of HA of average MW 150000 Da. The degree of substitution with thiol groups in H-HA-SH was 10%.

Synthesis of HA-BP derivatives. HA-BP derivatives were synthesised from L-HA and H thiolated HAs (HA-SH) via photo induced thiol-ene addition (Scheme 1) as reported previously.(*37*) They were abbreviated as L-HA-BP and H-HA-BP, respectively. In brief, acrylated BP **2** (57.8 mg, 0.2 mmol) was added to 200 mg of L-HA HA-SH or H-HA-SH in 12 mL degassed distilled water in order to obtain BP-to-thiol molar ratios of 4:1. Subsequently, 4 mg of Irgacure® 2959 was added and the mixture was stirred for 10 min under ultraviolet light (36 W UV timer lamp, CNC international BV, Netherlands). Thereafter, the mixture was dialysed against 0.1 M NaCl at pH 3.5 (MW cutoff of 3.5 kDa) and subsequently dialysed (48 h) against distilled water at pH 3.5 twice. The solution was neutralised to pH 7.4 and lyophilised. The resulting polymers were analysed by ^{1}H NMR and ^{31}P NMR and elemental analysis (colorimetric spectrophotometric method by OEA Labs).. Specifically, ^{1}H NMR peaks corresponding to the native HA protons (such as acetamide protons at 1.9 ppm; 2', 3', 4', 5' and 6'-protons of the HA disaccharide unit between 3.2–4.0 ppm as well as anomeric 1'-protons at 4.4 ppm) were compared with peaks corresponding to the methylene protons 2 and 3 of the grafted side chains. The peak at 2.2 ppm corresponds to two methylene protons $-CH_2C(OH)(PO_3H_2)_2$ that are adjacent to a bridging carbon of the BP group.

Synthesis of polyvinyl alcohol-BP (PVA-BP) derivatives. Thiolated PVA was first prepared according to a previously established protocol.(*38*) The degree of thiolation in PVA-SH was 4.5% (i.e. on an average, 16.2 out of 360 monomer units were thiolated in PVA of average MW 16000 Da). PVA-SH (35.3 mg, 32.4 μmol of –SH groups) was dissolved in 7 mL of degassed distilled water and acrylated BP **2** (9.4 mg, 32.4 μmol) was added to the solution. Subsequently, 4 mg of Irgacure® 2959 was added and the mixture was stirred for 10 min under ultraviolet light (36 W UV timer lamp, CNC international BV, Netherlands). Thereafter, the mixture was dialysed against distilled water three times. The dialysed solution was lyophilised to give 32 mg of PVA-BP (72% yield). The resulting polymer was analysed by ^{1}H NMR and ^{31}P NMR. ^{1}H NMR showed that one BP group was linked to each thiol group (Figure S1).

Fluorescent labelling of HA derivatives. Fluorescein B isothiocyanate (FITC) was linked to hydrazide-functionalised HA derivatives of L-HA and H-HA (L-HA-hy and H-HA-hy, respectively). Fluorescent labelling of bisphosphonated HA was performed analogously starting with HA derivatives dually functionalised with hydrazide and BP groups (L-HA-hy-BP and H-HA-hy-BP). Initial modification of either native HA or HA-BP with hydrazide groups was first accomplished according to our previously published protocol.(*39*) First, 20 mg each of each HA derivative (L-HA-hy and H-HA-hy; L-HA-hy-BP and H-HA-hy-BP) (Scheme S2) was dissolved in deionised water at concentrations of 12 mg/mL and 4 mg/mL, respectively. The pH of the obtained solutions was adjusted to 8 with 1 M NaOH. Then, 0.8 mg of FITC (*40*) was dissolved in 100 μL of dry methanol and added to the basified solution of HA-hydrazide derivative, corresponding to 0.03 molar equivalents of FITC with respect to the number of HA disaccharide units. The reaction mixture was stirred overnight in dark at room temperature (RT) and then dialysed against acidified water (pH 3.5) containing 0.1 M NaCl, followed by dialysis against acidified water twice. Dialysis tubes with a molecular weight cut-off of 3500 Da were used for H-HA-hy and H-HA-hy-BP, whereas dialysis tubes with a molecular weight cut-off of 1000 Da were used for L-HA-hy and L-HA-hy-BP. After freeze-drying the dialysed solutions, the following FITC-labelled derivatives were obtained: 10.7 mg (51.4% yield) of L-HA-hy, 15.3 mg (73.6% yield) of H-HA-hy, 11.5 mg (57.5% yield) of L-HA-hy-BP and 20 mg (100% yield) of H-HA-hy-BP.

Cell culture. Cells from the murine monocyte cell line RAW 264.7 were differentiated into osteoclast-like cells by addition of murine RANKL. In brief, the cells were grown in α-minimum essential medium (α-MEM, Gibco) supplemented with 10% foetal calf serum (FCS) (Gibco) with 50 μg/mL gentamycin at 37°C in a humidified atmosphere of 5% CO_2. In order to initiate the process of osteoclast formation, the cells were seeded (0.8 mL) in 8-well Lab-Tek chamber slides (BD Biosciences, Sweden) at a density of 2×10^3 cells

per chamber and cultured twice over a period of 5 days in a medium containing 20 ng/mL of murine RANKL (Peprotech, UK). On the 6th day, the induced cells were washed and treated with the compounds as described in Table 1. Human buffy coats from anonymous donors were provided by the Uppsala Hospital Blood Bank following a protocol approved by the research and ethical advisory committee. To isolate PBMCs, the buffy coats were diluted 1:1 (v/v) in warm PBS, layered over Ficoll-Paque Premium solution (GE Healthcare, Uppsala, Sweden) and centrifuged (400 g for 35 min) without brake. The PBMC layer was collected and washed in volumes of PBS, isolated by centrifugation (100 g) and resuspended in α -MEM containing 10% (v/v) FCS. Granulocyte contamination of PBMC was reduced to less than 1% by performing 2 additional Ficoll-Paque separations. Soluble human receptor activator of nuclear factor kappa-B ligand (RANKL) and recombinant human macrophage colony-stimulating factor (hM-CSF) were purchased from PeproTech (U.K.) and reconstituted in the medium at final concentrations of 40 ng/mL and 20 ng/mL, respectively. Cells were seeded at a total density of 5000 cells/cm^2, yielding a final seeding density of 1750 cells in 0.2 mL medium in each well of a 96 well plate. Cells were induced for 4 weeks with medium changes every 3 days. At 4 weeks, the induced cells were washed and treated with the compounds as described in Table 1. Tartrate-resistant acid phosphatase (TRAcP) activity was measured using a leukocyte acid phosphatase kit (Sigma). MC3T3-E1 pre-osteoblasts were obtained from ATCC and cultured in maintenance medium (α-MEM) (v/v) with 10% FCS and 1% penicillin-streptomycin at 37°C in a humidified atmosphere of 5% CO_2.

In vitro osteoclastogenesis. RAW 264.7 cells (0.8 mL/well) at a plating density of 5000 cells/cm^2 were seeded in 8-well Lab-Tek chamber slides at a final plating density of 2 × 10^3 cells per chamber and induced twice over a period of 5 days in the presence or absence of 20 ng/mL of RANKL (Peprotech, UK). On the 6th day, the induced cells were treated with the compounds as described in Table 1. After 24 h, the cells were TRAP-stained using a commercially available kit (Sigma Aldrich, St. Louis, MO, USA). Cell nuclei were stained using 300 nM 4´,6-diamidino-2-phenylindole dihydrochloride (DAPI) and then visualised using fluorescence microscopy. Tartrate resistant acid phosphatase (TRAP) that is a known osteoclast biomarker was used to identify mature bone resorbing cells. TRAP positive multinucleated cells (TPMCs) were defined as cells having 3 or more nuclei in addition to dark brown intracellular staining., As additional controls, these cells were incubated with native HA of H-HA and L-HA. For statistical evaluation, the cell numbers of mature osteoclasts was counted using four different fields of view and repeated four times.

Total cellular metabolic activity assay using AlamarBlue®. RAW 264.7 and MC3T3-E1 cells were trypsinised and suspended in fresh media aliquoted (0.2 mL) to contain 5 × 10^3 cells/cm^2 in a 96 well plate. A fresh working solution of 10% AlamarBlue®® was prepared by mixing 1 ml AlamarBlue® stock solution with 9 ml media (DMEM and α-MEM with 10% FCS but without phenol red and serum) and wrapped in foil until further use. The media were discarded and 1 ml of medium containing AlamarBlue® was added to the test wells and incubated at 37°C for 90 min. Thereafter, 100 µL of this working solution (after incubation with cells) was transferred to a 96-well plate and fluorescence was determined on an Infinity plate reader with excitation at 560 nm and emission at 590 nm, followed by subtraction of background values. The seeding density and medium volume were kept constant in all groups.

Confocal microscopy. Immunostaining was performed 24 h after incubating with the samples from Table 1 labelled with FITC. In brief, the cells were washed with PBS, fixed with 4% paraformaldehyde and permeabilised in 0.01% Triton-PBS. Nonspecific binding sites were blocked with the addition of 10% goat serum for 1 h. To examine the role of the CD44 receptor in the uptake process, the cells were treated with a monoclonal antibody specific for the mouse CD44 receptor and counter stained with a rhodamine-linked secondary antibody for visualisation. L-HA-hy-BP and H-HA-hy-BP were labelled with FITC as described above to follow the polymer linked-BP. DAPI was used to stain the multiple nuclei. The cells were incubated for 60 min at RT with monoclonal rat anti-mouse anti-CD44 antibody (50 µL/well, 1:100 diluted 1% donkey serum with PBS) and subsequently incubated with secondary fluorescent antibody (50 µL/well, 1:200 diluted donkey anti-rat IgG conjugated with rhodamine; (Molecular Probes) at RT for 30 min in darkness. Cell nuclei were stained using DAPI for 30 min at RT in dark. The cells were washed with PBS and then mounted in Vectashield mounting fluid (Vector). Fluorescence images were acquired using a Zeiss confocal laser-scanning microscope. Images were quantified using Image J (Free source software from NIH).

Statistical analysis. All quantitative experiments were performed in triplicate and the data are shown as the mean ± standard deviation of one representative experiment. The results are expressed as mean ± SD. Statistical significance was calculated with Student's *t*-test for unpaired samples using the SPSS statistical analysis software. *p* Values less than 0.05 were considered significant.

C. Results

BP groups were linked to HA to form HA-BP. HA of MW 8 and 150 kD (designated as L-HA and H-HA, respectively) was functionalised with BP groups in two steps according to the reported procedure.(*37*) In brief, native HAs were first modified with thiol groups using linker **1,** which facilitated synthesis of L-HA-SH and H-HA-SH, respectively (Scheme 1). In both derivatives, the degree of substitution with thiol groups was approximately 10%. Subsequently, photo-initiated thiol-ene addition of thiol groups to pamidronate acrylamide **2** resulted in the bisphosphonated analogues L-HA-BP and H-HA-BP. On average, 2.5 and 3 molecules of acrylated BP molecules were added per thiol group in L-HA-BP and H-HA-BP, respectively, as was judged from ^{1}H NMR analysis (Figure 1). HA functionalisation with BP groups was confirmed by appearance of methylene protons 1 adjacent to the bridging carbon of the BP group (see structure in Figure 1A for designation). The degree of substitution with BP's (DS_{BP}) was found to be 25% for L-HA-BP according to the comparative integration of this peak and the singlet of HA acetamide protons at 1.9 ppm. Moreover, a characteristic singlet phosphorus peak at 18.7 ppm was observed for the attached BP's in ^{31}P NMR spectra (Figure 1B). ^{1}H NMR and ^{31}P NMR spectra of H-HA-BP were similar to those of the L-HA-BP analogue, indicating that the conjugation efficiency did not depend on the MW of HA. Elemental analysis of HA-BP derivatives showed of 3.2% phosphorous and 0.7% sulphur content indicating that approximately 2.3 bisphosphonate groups were linked to each thiol group.

Figure 1. Figure 1. (A) Synthesis scheme for BP-functionalised HA (L-HA-BP and H-HA-BP). (B) ^{1}H NMR and (C) ^{31}P NMR spectra of the L-HA-BP derivative in D_2O.

BP-linked HA exhibits anti-proliferative effects on murine osteoclast-like cells. The results in Figure 2 show that RAW 264.7 cells induced with 20 ng/mL RANKL twice for 5 days formed giant TPMCs mimicking osteoclasts. We quantified the effect of H-HA and L-HA as well as H-HA-BP and L-HA-BP in comparison with parent pamidronate on the survival and proliferation of RANKL-induced murine osteoclast-like cells using a standard TRAP assay.(*42*) L-HA-BP at a concentration of 100 μM exhibited the highest toxicity by reducing over 90% of the osteoclast-like cells, whereas H-HA-BP exhibited approximately 60% toxicity. In contrast, L-HA, H-HA and unmodified BP demonstrated only limited (approximately 35%) reduction in osteoclast-like cell numbers compared with the untreated control within 24 h. Hydrazide-linked HA of both molecular weights without BP's also showed between 30-40% toxicity by themselves. To quantify the effect of H-HA and L-HA without linked BP's on the survival of osteoclasts, HA of 7.5 and 150 kD was dissolved and added at 100 μM concentration to the culture of RANKL-induced RAW 264.7 cells. No significant effect of native L-HA and H-HA on cell proliferation was observed. In addition, there was no direct evidence of involvement of L-HA and H-HA on osteoclastogenesis at 100 μM concentrations. (Figure 2 & 3)

Figure 2. (A) Effect of BPs on murine osteoclast-induced TRAP activity. RAW 264.7 cells were induced with (20 ng/mL) RANKL for 5 days. Subsequently they were treated with BPs for 24 h. TRAP activity was measured as described in 'Materials and Methods'. The images show the formation of giant multi-nucleated cells indicating the presence/absence of osteoclast-like cells. A. H-HA (avg. MW= 150 kD); B. L-HA (avg. MW = 7.5 kD); C. Control; D. H-HA-BP (avg. MW = 150kD); E. L-HA-BP (avg. MW = 7.5 kD); F. Free BP. **(B)** Image analysis was performed on the different groups and quantified as represented in the graph. Statistical significance was calculated with Student's *t*-test. P value < 0.01 when compared across the groups.

Figure 3. (A) Effect of BPs on human osteoclast-induced TRAP activity. PBMC's were induced with 40 ng/mL RANKL and 40 ng/mL M-CSF for 4 weeks. Subsequently they were treated with BPs for 24 h. TRAP activity was measured as described in 'Materials and Methods'. The images show the formation of giant multi-nucleated cells indicating the presence/absence of osteoclast-like cells. A. H-HA (avg. MW= 150 kD); B. L-HA (avg. MW = 7.5 kD); C. Control; D. H-HA-BP (avg. MW = 150kD); E. L-HA-BP (avg. MW = 7.5 kD); F. Free BP. **(B)** Image analysis was performed on the different groups and quantified as represented in the graph. P value < 0.01 when compared across the groups. Images with DAPI staining for nuclei of human osteoclasts were used only for analysis and representative images are presented without nuclear staining to improve clarity. Scale bars represent 200 μm. Statistical significance was calculated with Student's *t*-test. P value < 0.01 when compared across the groups.

.

To investigate if the drug-linked polymer had any dose-dependent toxicity towards human osteoclasts, we exposed mature osteoclasts at week 4, with an increasing dosage of BP-linked polymer (0, 1, 10, 50 or 100 μM) for 24h and performed TRAcP staining on the cells post-fixation with 4% PFA. The cells showed increasing dose-dependent toxicity up to 100 μM concentration.

Figure 4. Effects of HA-linked bisphosphonates (0, 1, 10, 50 or 100 μM) on osteoclast differentiation. Human osteoclasts were treated with different concentrations of bisphosphonates (0, 1, 10, 50 or 100 μM) for 24h and counted both the number of osteoclasts and large osteoclasts after 4 weeks of culture. Results are shown as means ± SD for four independent experiments. P>0.05 and represents significant difference from control osteoclasts (≥2 nuclei).

In addition, we examined whether linking of the BP moiety to a synthetic polymer, devoid of cell surface receptor recognition molecules such as PVA of similar MW, would have any effect that mimics the effect of L-HA-BP on osteoclast-like cells. **(SI. Table 1)**
L-HA-BP at a concentration of 100 μM exhibited the highest toxicity by reducing over 90% of the murine osteoclast-like cells as well as human osteoclasts, whereas H-HA-BP exhibited approximately 60% toxicity. In contrast, L-HA, H-HA and unmodified BP demonstrated only limited (approximately 35%) reduction in osteoclast numbers compared with the untreated control within 24 h. To quantify the effect of H-HA and L-HA without linked BP's on the survival of both murine and human osteoclasts, HA of 7.5 and 150 kD was dissolved and added at 100 μM concentration to the culture of RANKL-induced RAW 264.7 cells or human osteoclast cultures. No significant effect of native L-HA and H-HA on cell proliferation was observed. In addition, there was no direct evidence of involvement of L-HA and H-HA on osteoclastogenesis at 100 μM concentrations. In addition, we examined whether linking of the BP moiety to a synthetic polymer, devoid of cell surface receptor recognition molecules such as PVA of similar MW, would have any effect that mimics the effect of L-HA-BP on osteoclasts. **(SI. Table 1)** The PVA-BP derivative was obtained analogously to HA, that is via thiol-ene addition reaction of thiolated PVA (PVA-SH) to pamidronate acrylamide **2** (synthesis scheme and NMR characterisation are given in Supporting Information). We found that PVA-BP does not elicit any detectable toxicity towards osteoclasts. (Figure S3) RAW 264.7 cells were cultured and observed separately in a medium without RANKL alongside the differentiated osteoclast-like cells to ascertain the effect of the compounds on undifferentiated cells. We found that only L-HA-BP presented minor toxicity to the undifferentiated monocytes/macrophages assessed through cell counting when together in culture with differentiated cells. To ascertain the effect of the fluorescent labelling of the compounds, we repeated the experiment as described above and observed that there was no difference between L-HA-hy-BP and L-HA-BP in terms of reduction of osteoclast numbers. **(SI. 4)**

BP-linked HA is selective in toxicity towards osteoclasts. Figures 3 and 4 show that the toxicity exhibited by L-HA-hy-BP and H-HA-hy-BP towards osteoclasts was not replicated towards other cell types. The effects of these HA-derivatives were investigated by testing them against undifferentiated RAW 264.7 cells and a primary murine pre-osteoblast clone (MC3T3-E1). All compounds (L-HA-hy-BP, H-HA-hy-BP, H-HA, L-HA, free BP with concentrations normalised to the same BP concentration) and untreated controls were presented to both cell types for a 24-h period at the same concentrations as presented to the osteoclast-like cell cultures.

Figure 5. Effect of BP-linked compounds on pre-osteoblasts (A) and murine macrophages (B). MC3T3-E1 cells were exposed to BP-containing and BP-free compounds and evaluated for cytotoxicity using the AlamarBlue® assay as described above (A). RAW 264.7

cells were exposed to BP-containing and BP-free compounds for 24 h and evaluated for cytotoxicity using the AlamarBlue® assay as described above. Data are expressed as the mean ± S.D. of triplicate cultures. The experiment was performed three times, with similar results obtained in each experiment. Statistical significance was calculated with Student's *t*-test. P value < 0.01 when compared across the groups.

The metabolic activity of the cells was assessed using the AlamarBlue® assay and plotted as cell survival compared with untreated control. Differentiated osteoclasts demonstrate variable responses when incubated with AlamarBlue® and therefore TRAP assay showed the most reliable method to testing osteoclasts, whereas the undifferentiated cells show measureable response towards AlamarBlue®. In a similar experiment, native L-HA and H-HA exhibited approximately 50% toxicity towards both pre-osteoblasts and undifferentiated murine macrophages in 24 h tested at concentrations mentioned for the above compounds. In contrast, the BP-functionalised derivatives were significantly less toxic towards both these cell types. Free pamidronate, however, showed approximately 70% toxicity towards both cell types during the 24-h incubation period. Thus, the inhibitory effect of L-HA-BP and H-HA-BP on the proliferation of murine osteoclasts is specific and does not negatively influence MC3TC-E1 cells.

L-HA-BP conjugates selectively undergo uptake in RAW 264.7 cells induced by RANKL. To further examine the mechanism of cellular entry, RAW 264.7 cells were exposed to fluorescently labelled HA derivatives after a 5-day induction period by RANKL. For fluorescent labelling, hydrazide or dual hydrazide and BP derivatives of 8 and 150 kD were prepared (designated as L-HA-hy, H-HA-hy, L-HA-hy-BP and H-HA-hy-BP, respectively). The hydrazide functionality was introduced specifically to react with the isothiocyanate reactive group (-N=C=S) of FITC. The aforementioned groups of compounds were added to the cells and incubated for a period of 12 h, since most osteoclast-like cells showed toxic response towards the BP-linked HA only around 24 h. After 12 h, these cells were examined for the transport of BP's across the membrane. It was observed that only multinucleated osteoclast-like cells stained positive for uptake and the polymer was observed to localise in vesicles inside the cell. Free FITC did not localise into vesicles. In addition, there was no uptake of any of the polymer-drug conjugates in the undifferentiated murine monocytes/macrophages as revealed by confocal microscopy results, thereby indicating selective uptake. H-HA-hy-BP did not show any visible uptake in 12 h and appeared to adhere to the cell surface (Figure 5).

Figure 6. Cellular uptake of HA-hy-BP-FITC in murine osteoclasts. RAW 264.7 cells were stimulated with RANKL (20 ng/mL) for 5 days to differentiate into osteoclast-like cells and incubated in the presence of FITC-labelled H-HA-hy-BP (A). Scale bar for (A) represents 50μm (B) L-HA-hy-BP. Scale bar for (A) represents 100μm. Blue colour represents DAPI staining of the multiple nuclei in each cell body. Compounds penetrate the cell membrane with L-HA-hy-BP and remain at cell surface with H-HA-hy-BP at 100 μM concentration.

D. Discussion

In this study, we covalently derivatised HA with a BP moiety to form a potent and biodegradable drug-polymer complex. To verify whether the potency and specificity of the drug against osteoclasts was enhanced, we challenged an in vitro osteoblast and/or osteoclast cell culture model with this new adduct.

We explored the idea of linking the BP drug to HA in order to increase the probability of the drug-linked polymer to be internalised through processes such as receptor-mediated endocytosis through CD44 (receptor for hyaluronan), clathrin-mediated pits and pinocytosis.(*43*) It has been suggested in previous work that low molecular weight HA can penetrate the cell with greater efficiency using receptor mediated endocytosis compared to high molecular weight HA.(*44*) We made an important observation that when the drug was linked to HA, the toxicity of the drug towards osteoclasts increased, which could be attributed to enhanced uptake. The polymer-drug conjugate also demonstrated concentration dependent toxicity, implying that dosage could be controlled and even concentrations as low as 10 μM could elicit the desired pharmacological response in vitro. The free drug and HA polymer lacking the BP moiety itself did not impose any significant toxic effect on the osteoclasts. We noted that the hydrazide-modified compounds did elicit some toxicity of their own and can be attributed to the presentation of unreacted hydrazide groups as an irritant. Significantly, the polymer-linked drugs did not significantly affect undifferentiated monocytes. This corroborates with improved uptake of L-HA HA by endocytosis.(*44*). It has been previously demonstrated that osteoblasts show low expression levels of CD44, whereas osteocytes and osteoclasts show higher expression levels of CD44 receptors.(*36*) BP-based drugs are known to inhibit mature osteoclasts from attaching to the bone surface by altering the cytoskeleton and subsequent loss of the ruffled borders, thereby slowing down resorption.(*45*) In order to verify if the effect is replicable with a drug delivery vehicle that does not present suitable ligands for receptor-mediated uptake, we used bisphosphonated PVA. Indeed, this adduct had no detectable effect on the survival of osteoclasts. Another important requirement for new-generation drugs is non-toxicity towards unrelated cell types. Here we observed that the drug-linked polymer does not affect the growth or proliferation of osteoblasts, which possess the inherent mechanisms to remineralise and heal defects in bone. This makes the polymer-linked drug a multimodal vehicle, where BP targets bone and HA targets specific cell surface receptors present on osteoclasts. Further, we investigated the transport of the drug-linked polymer L-HA-BP into mature osteoclasts to rule out any involvement of toxicity arising through the interaction of L-HA-BP merely with the cell surface. We equipped the polymer with a fluorescent probe to locate its movement or attachment and performed the experiment under the same conditions as described before. Although only a few mature osteoclasts survived incubation with the drug for 12 h, the ones that survived were fixed and stained with DAPI to locate the nuclear body. We could distinctly locate pockets inside the multi-nucleated osteoclasts with the fluorescent polymer of L-AH. In the case of monocytes, we demonstrated that fluorescence appeared only at the cell surface and not inside the cell, reiterating our observations that the drug-linked polymer shows high specificity towards multinuclear mature osteoclasts only. This demonstrates the preference of the polymer-drug conjugate towards mature osteoclasts and not towards other cell types. We speculate that this could be possibly mediated through the interaction of the complex with CD44 receptors or other HA receptors, allowing higher possibility for the drug to be taken into the osteoclast cell body. It has been suggested that efficient treatment of skeletal disorders such as osteoporosis ideally requires the development of smart delivery strategies that can target osteoclasts without disturbing other functioning cell

types.(*46*) This paves the way for selective and higher levels of uptake by osteoclasts, lower doses and reduced side effects.

D. Conclusion

The in vivo scenario related to bone renewal is complex with cellular cross talk, and built-in mechanisms have been developmentally incorporated that allow the cells to survive higher levels of stress. Extreme stress changes the way cells orchestrate bone turnover, which cannot be rebalanced without drug intervention. The drugs available at present are capable of treating osteoporosis; however, they are associated with severe side effects. We have developed a HA-linked BP derivative and demonstrated increased specific targeting of the drug towards osteoclasts, thereby offering unaffected osteoblasts a chance to rebalance the process of mineralisation and resorption. We reason that by linking the drug to an efficient carrier, the required dose of the drug can also be lowered significantly. Hence, HA-linked BP may offer the opportunity for long-term treatment of patients with osteoporosis with higher compliance rates. Future work should explore in depth the mechanisms involved in signalling of such complexes in cells to better understand the cellular response towards such 'smart targeting vehicles'. We expect that this type of targeted delivery system can be extended to other classes of drugs in the future.

Acknowledgements

The research leading to these results has received funding from the European Community's Seventh Framework Programme (MultiTERM, Grant no: 238551).
Advice and Sharing of Expertise
We extend our gratitude to Mr Fredrik Edin, Department of Surgical Sciences, Otolaryngology and Head & Neck Surgery, Akademiska Sjukhuset, Uppsala, for his time and advice on microscopic evaluation of the materials. We also extend our gratitude to Dr. X. Lu for his help and insights while reviewing the figures.
The authors declare no competing financial interest.

References

1. B. L. Riggs, L. J. Melton, 3rd, The worldwide problem of osteoporosis: insights afforded by epidemiology. *Bone* **17**, 505S-511S (1995).
2. J. A. Kanis *et al.*, SCOPE: a scorecard for osteoporosis in Europe. *Archives of osteoporosis* **8**, 144 (2013).
3. O. Strom *et al.*, Osteoporosis: burden, health care provision and opportunities in the EU: a report prepared in collaboration with the International Osteoporosis Foundation (IOF) and the European Federation of Pharmaceutical Industry Associations (EFPIA). *Archives of osteoporosis* **6**, 59-155 (2011).
4. H. N. Viswanathan *et al.*, Direct healthcare costs of osteoporosis-related fractures in managed care patients receiving pharmacological osteoporosis therapy. *Applied health economics and health policy* **10**, 163-173 (2012).
5. P. A. Downey, M. I. Siegel, Bone biology and the clinical implications for osteoporosis. *Physical therapy* **86**, 77-91 (2006).
6. H. K. Datta, W. F. Ng, J. A. Walker, S. P. Tuck, S. S. Varanasi, The cell biology of bone metabolism. *Journal of clinical pathology* **61**, 577-587 (2008).
7. D. W. Buck, G. A. Dumanian, Bone Biology and Physiology: Part I. The Fundamentals. *Plast Reconstr Surg* **129**, 1314-1320 (2012).
8. F. Shapiro, Bone development and its relation to fracture repair. The role of mesenchymal osteoblasts and surface osteoblasts. *European cells & materials* **15**, 53-76 (2008).
9. T. Garcia *et al.*, Behavior of osteoblast, adipocyte, and myoblast markers in genome-wide expression analysis of mouse calvaria primary osteoblasts in vitro. *Bone* **31**, 205-211 (2002).
10. R. Baron, M. Zaidi, Bone Cell Biology - Osteoclasts - Session-5. *Bone* **17**, S55-S56 (1995).
11. B. F. Boyce, Advances in osteoclast biology reveal potential new drug targets and new roles for osteoclasts. *Journal of bone and mineral research : the official journal of the American Society for Bone and Mineral Research* **28**, 711-722 (2013).
12. J. R. Edwards, G. R. Mundy, Advances in osteoclast biology: old findings and new insights from mouse models. *Nature reviews. Rheumatology* **7**, 235-243 (2011).
13. M. J. Cielinski, S. C. Marks, Jr., Understanding bone cell biology requires an integrated approach: reliable opportunities to study osteoclast biology in vivo. *Journal of cellular biochemistry* **56**, 315-322 (1994).
14. K. Pervaiz, A. Cabezas, K. Downes, B. G. Santoni, M. A. Frankle, Osteoporosis and shoulder osteoarthritis: incidence, risk factors, and surgical implications. *Journal of shoulder and elbow surgery / American Shoulder and Elbow Surgeons ... [et al.]* **22**, e1-8 (2013).
15. C. Wilson, Osteocytes, RANKL and bone loss. *Nature reviews. Endocrinology* **7**, 693 (2011).
16. S. A. Lloyd *et al.*, Administration of high-dose macrophage colony-stimulating factor increases bone turnover and trabecular volume fraction. *J Bone Miner Metab* **27**, 546-554 (2009).
17. M. N. Weitzmann, The Role of Inflammatory Cytokines, the RANKL/OPG Axis, and the Immunoskeletal Interface in Physiological Bone Turnover and Osteoporosis. *Scientifica* **2013**, 125705 (2013).
18. S. Yano, [Clinical usefulness of bone turnover markers in the management of osteoporosis]. *Rinsho byori. The Japanese journal of clinical pathology* **61**, 852-859 (2013).
19. K. Henriksen, J. Bollerslev, V. Everts, M. A. Karsdal, Osteoclast activity and subtypes as a function of physiology and pathology--implications for future treatments of osteoporosis. *Endocrine reviews* **32**, 31-63 (2011).
20. W. F. Lems, P. Geusens, Established and forthcoming drugs for the treatment of osteoporosis. *Curr Opin Rheumatol* **26**, 245-251 (2014).
21. N. Miyakoshi, [New Development in Osteoporosis Treatment. Intermittent long-term administration of intravenous bisphosphonates for treatment of osteoporosis]. *Clinical calcium* **24**, 93-99 (2014).
22. R. G. Russell, Bisphosphonates: the first 40 years. *Bone* **49**, 2-19 (2011).
23. R. G. Russell, N. B. Watts, F. H. Ebetino, M. J. Rogers, Mechanisms of action of bisphosphonates: similarities and differences and their potential influence on clinical

efficacy. *Osteoporosis international : a journal established as result of cooperation between the European Foundation for Osteoporosis and the National Osteoporosis Foundation of the USA* **19**, 733-759 (2008).

24. B. Jobke, P. Milovanovic, M. Amling, B. Busse, Bisphosphonate-osteoclasts: Changes in osteoclast morphology and function induced by antiresorptive nitrogen-containing bisphosphonate treatment in osteoporosis patients. *Bone* **59**, 37-43 (2014).
25. J. Gao *et al.*, Multi-target-directed design, syntheses, and characterization of fluorescent bisphosphonate derivatives as multifunctional enzyme inhibitors in mevalonate pathway. *Biochimica et biophysica acta* **1830**, 3635-3642 (2013).
26. M. A. Sillero *et al.*, Synthesis of ATP derivatives as compounds of the mevalonate pathway (isopentenyl di- and triphosphate; geranyl di- and triphosphate, farnesyl di- and triphosphate, and dimethylallyl diphosphate) catalyzed by T4 RNA ligase, T4 DNA ligase and other ligases Potential relationship with the effect of bisphosphonates on osteoclasts. *Biochemical pharmacology* **78**, 335-343 (2009).
27. P. Schwarz, N. R. Jorgensen, B. Abrahamsen, Status of drug development for the prevention and treatment of osteoporosis. *Expert opinion on drug discovery* **9**, 245-256 (2014).
28. K. Ganda, A. Schaffer, S. Pearson, M. J. Seibel, Compliance and persistence to oral bisphosphonate therapy following initiation within a secondary fracture prevention program: a randomised controlled trial of specialist vs. non-specialist management. *Osteoporosis Int* **25**, 1345-1352 (2014).
29. K. Makita *et al.*, Survey of the utility of once-monthly bisphosphonate treatment for improvement of medication adherence in osteoporosis patients in Japan. *Bone Miner Metab*, (2014).
30. G. A. Rodan, T. J. Martin, Therapeutic approaches to bone diseases. *Science* **289**, 1508-1514 (2000).
31. A. Outeirino-Fernandez, [Osteonecrosis of the jaw associated with bisphosphonate therapy in primary osteoporosis. Review of the literature]. *Anales del sistema sanitario de Navarra* **36**, 87-97 (2013).
32. E. Cenni *et al.*, The Effect of Poly(D,L-Lactide-co-Glycolide)-Alendronate Conjugate Nanoparticles on Human Osteoclast Precursors. *Journal of Biomaterials Science-Polymer Edition* **23**, 1285-1300 (2012).
33. J. Kim *et al.*, Bone regeneration using hyaluronic acid-based hydrogel with bone morphogenic protein-2 and human mesenchymal stem cells. *Biomaterials* **28**, 1830-1837 (2007).
34. E. R. Bastow *et al.*, Hyaluronan synthesis and degradation in cartilage and bone. *Cellular and Molecular Life Sciences* **65**, 395-413 (2008).
35. H. Harada, M. Takahashi, CD44-dependent intracellular and extracellular catabolism of hyaluronic acid by hyaluronidase-1 and -2. *J Biol Chem* **282**, 5597-5607 (2007).
36. D. E. Hughes, D. M. Salter, R. Simpson, CD44 expression in human bone: a novel marker of osteocytic differentiation. *Journal of bone and mineral research : the official journal of the American Society for Bone and Mineral Research* **9**, 39-44 (1994).
37. M. R. Nejadnik *et al.*, Self-healing hybrid nanocomposites consisting of bisphosphonated hyaluronan and calcium phosphate nanoparticles. *Biomaterials* **35**, 6918-6929 (2014).
38. D. A. Ossipov, S. Piskounova, J. Hilborn, Poly(vinyl alcohol) cross-linkers for in vivo injectable hydrogels. *Macromolecules* **41**, 3971-3982 (2008).
39. D. A. Ossipov, S. Piskounova, O. P. Varghese, J. Hilborn, Functionalization of Hyaluronic Acid with Chemoselective Groups via a Disulfide-Based Protection Strategy for In Situ Formation of Mechanically Stable Hydrogels. *Biomacromolecules* **11**, 2247-2254 (2010).
40. M. Guan *et al.*, Directing mesenchymal stem cells to bone to augment bone formation and increase bone mass. *Nat. Med. (N. Y., NY, U. S.)* **18**, 456-462 (2012).
41. D. Steinmuller-Nethl *et al.*, Strong binding of bioactive BMP-2 to nanocrystalline diamond by physisorption. *Biomaterials* **27**, 4547-4556 (2006).
42. A. W. Kung *et al.*, Factors influencing diagnosis and treatment of osteoporosis after a fragility fracture among postmenopausal women in Asian countries: a retrospective study. *BMC women's health* **13**, 7 (2013).
43. L. G. Wu, E. Hamid, W. Shin, H. C. Chiang, Exocytosis and endocytosis: modes, functions, and coupling mechanisms. *Annual review of physiology* **76**, 301-331 (2014).
44. J. M. Cyphert, C. S. Trempus, S. Garantziotis, Size Matters: Molecular Weight Specificity of Hyaluronan Effects in Cell Biology. *International Journal of Cell Biology*.
45. M. Tsubaki *et al.*, Nitrogen-containing bisphosphonates inhibit RANKL- and M-CSF-induced osteoclast formation through the inhibition of ERK1/2 and Akt activation. *Journal of biomedical science* **21**, 10 (2014).
46. I. R. Reid *et al.*, Continuous therapy with pamidronate, a potent bisphosphonate, in postmenopausal osteoporosis. *The Journal of clinical endocrinology and metabolism* **79**, 1595-1599 (1994).

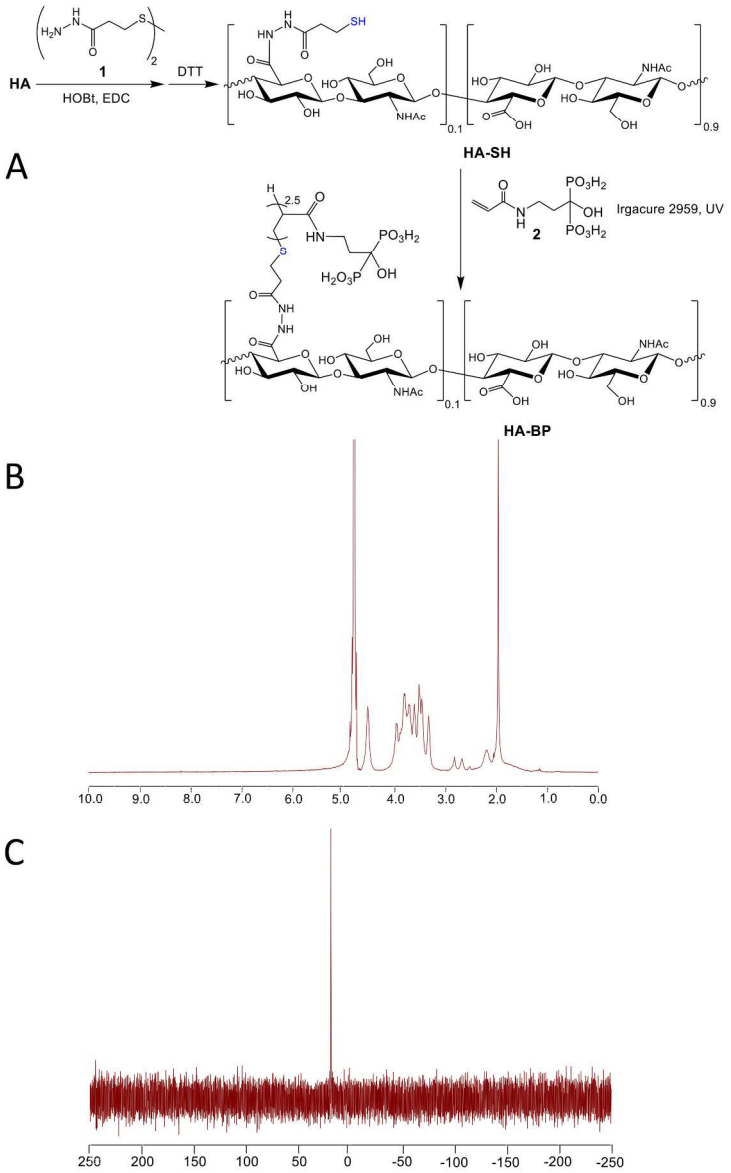

190x286mm (300 x 300 DPI)

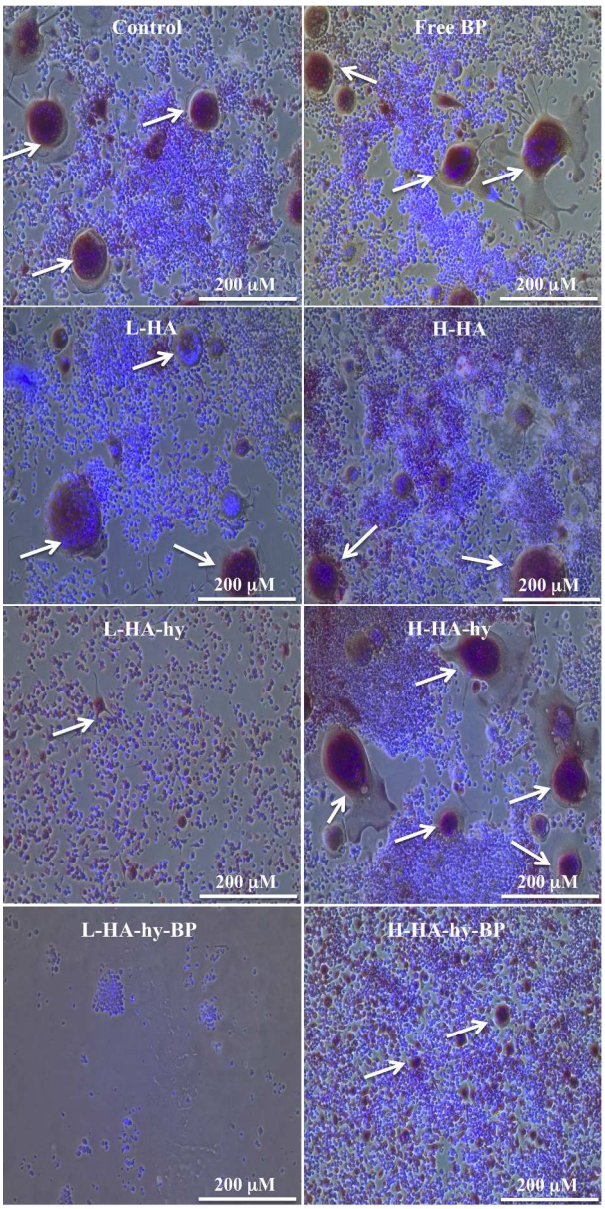

200x401mm (300 x 300 DPI)

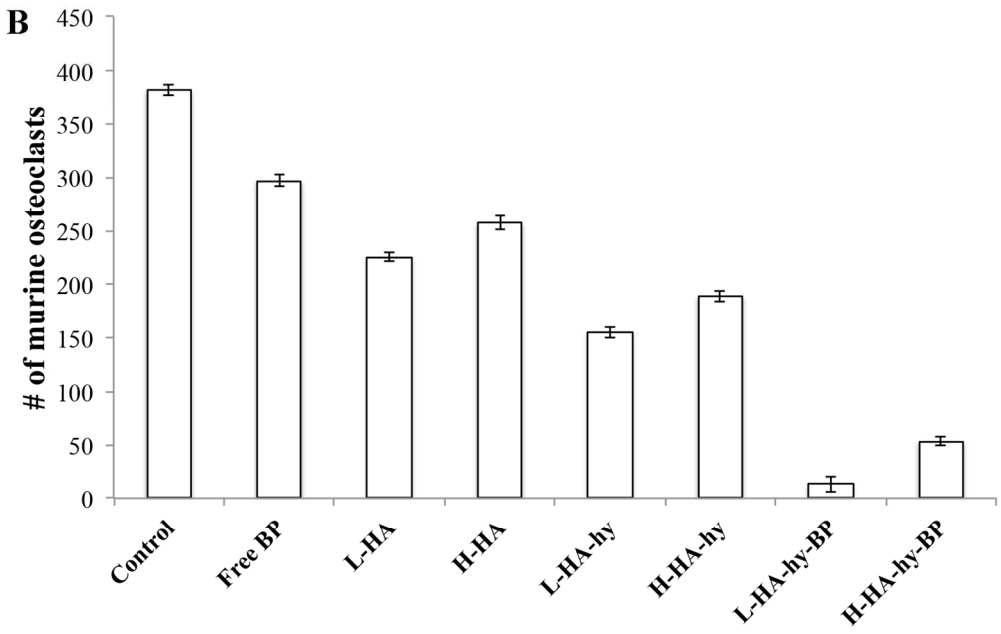

141x89mm (300 x 300 DPI)

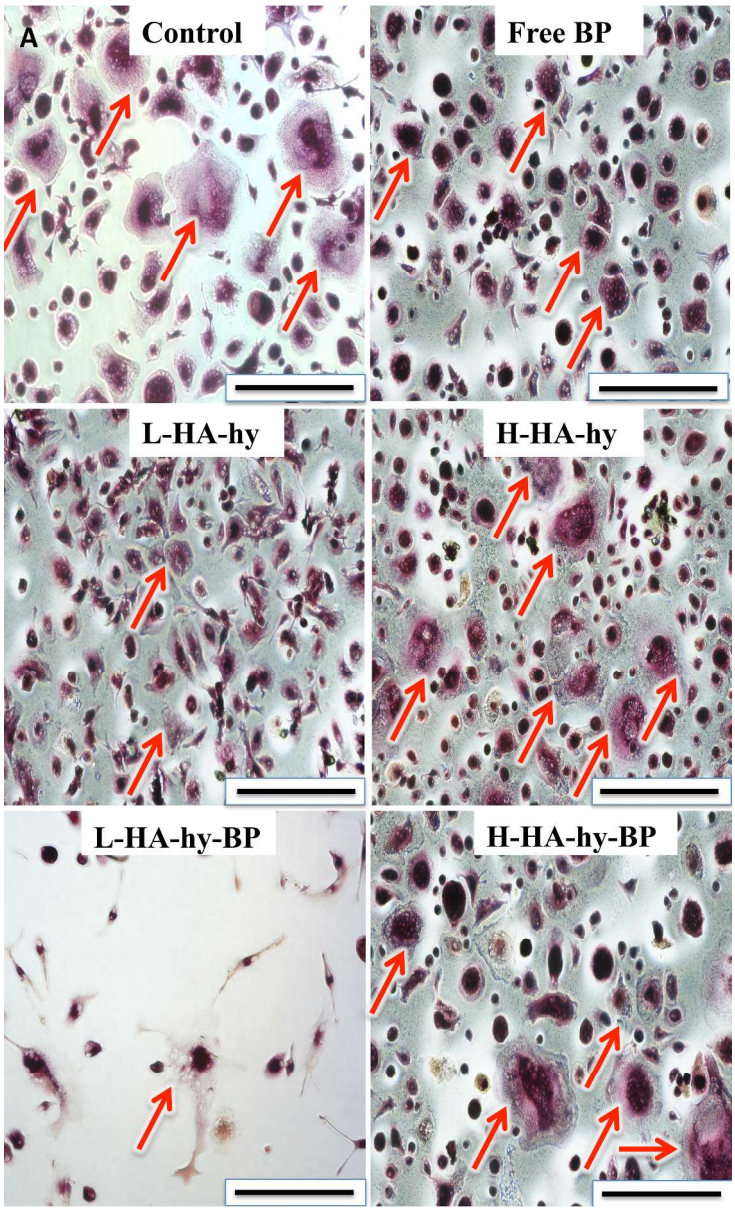

250x412mm (300 x 300 DPI)

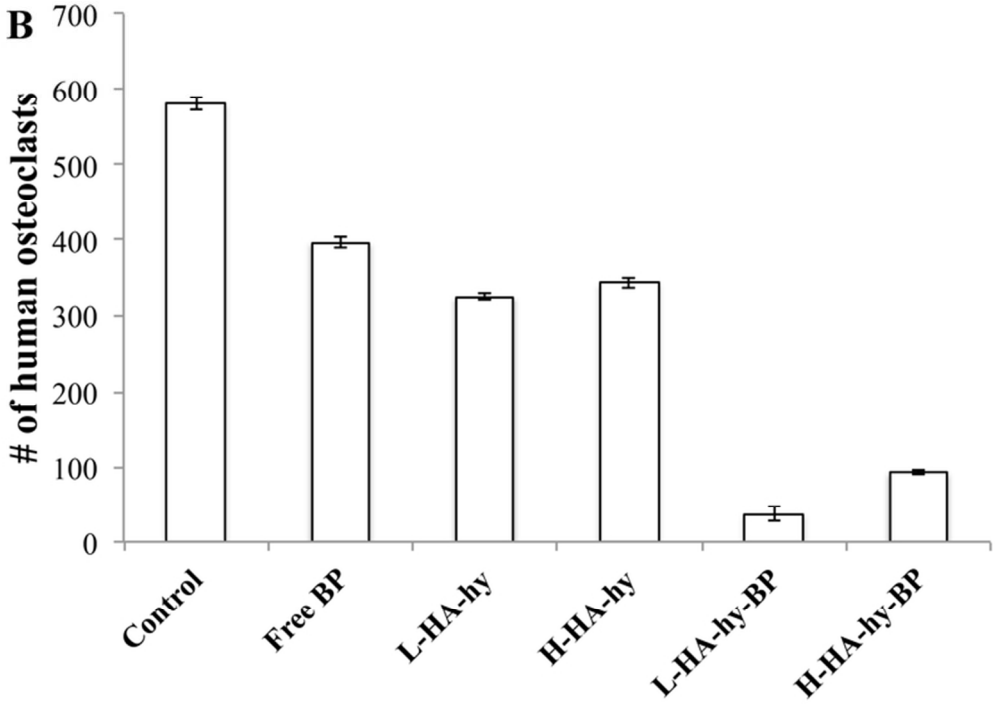

67x48mm (300 x 300 DPI)

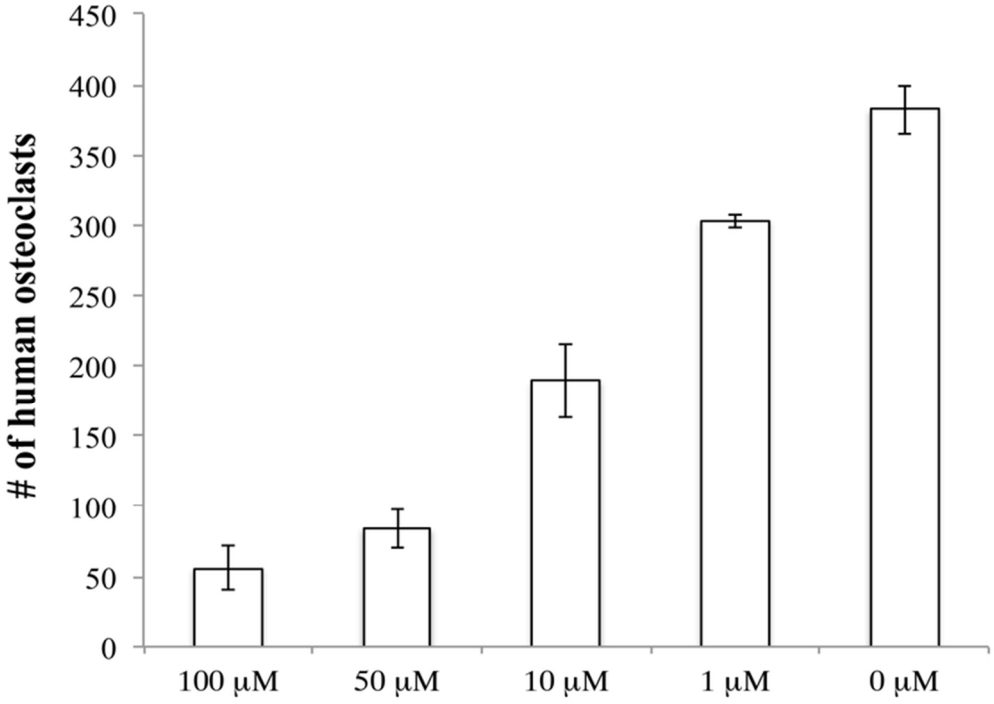

68x48mm (300 x 300 DPI)

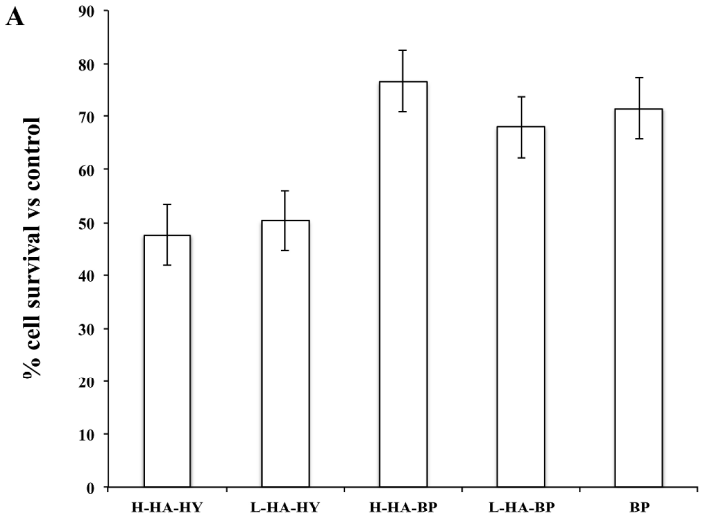

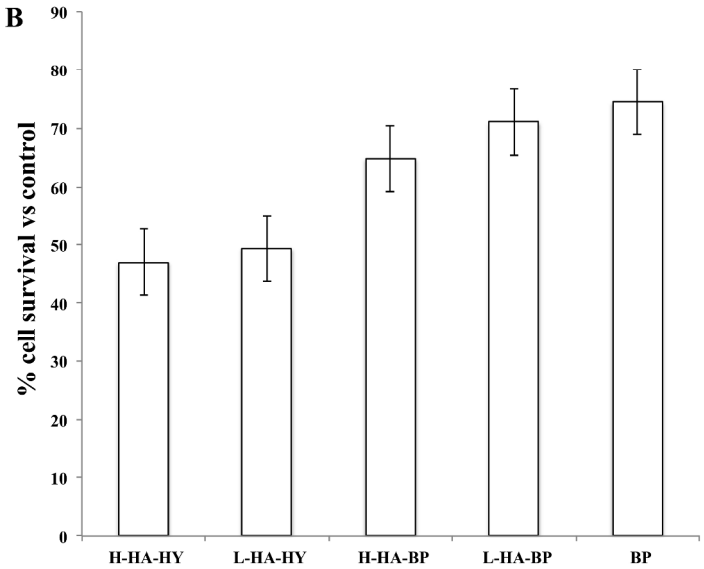

271x428mm (300 x 300 DPI)

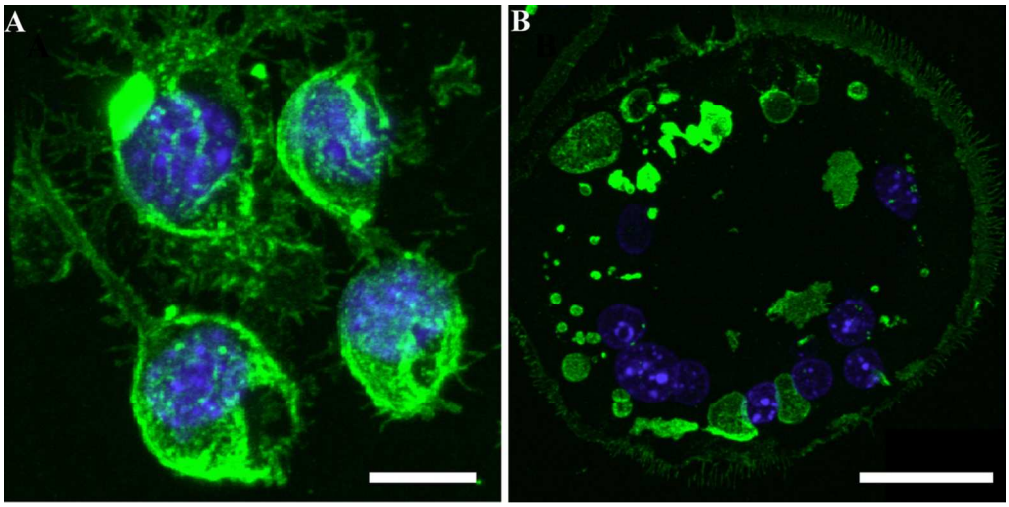

102x50mm (300 x 300 DPI)